ONLINE FIRST

This is a provisional PDF only. Copyedited and fully formatted versión will be made available at final publication

HISTOLOGY AND HISTOPATHOLOGY

ISSN: 0213-3911
e-ISSN: 1699-5848

Submit your article to this Journal (http://www.hh.um.es/Instructions.htm)

Upregulation of autophagy and glycolysis markers in keloid hypoxic-zone fibroblasts: Morphological characteristics and implications

Authors: Okuno Ryoko, Yuko Ito, Nabil Eid, Yoshinori Otsuki, Yoichi Kondo and Koichi Ueda

DOI: 10.14670/HH-18-005
Article type: ORIGINAL ARTICLE
Accepted: 2018-05-29
Epub ahead of print: 2018-05-29

Upregulation of autophagy and glycolysis markers in keloid hypoxic-zone fibroblasts: Morphological characteristics and implications

Okuno Ryoko[1], Yuko Ito[2]*, Nabil Eid[2], Yoshinori Otsuki[3], Yoichi Kondo[2] and Koichi Ueda[1]

[1]Plastic and Reconstructive Surgery Department, Osaka Medical College, Osaka, Takatsuki, Japan; [2]Department of Anatomy and Cell Biology, Division of Life Sciences, Osaka Medical College, Osaka, Takatsuki, Japan, [3]Osaka Medical College, Osaka, Takatsuki, Japan.

*Correspondence to Dr. Yuko Ito, Division of Life Sciences, Department of Anatomy and Cell Biology, Osaka Medical College, 2-7 Daigaku-machi, Takatsuki, Osaka 569-8686, Japan

E-mail: an1006@osaka-med.ac.jp

Fax: +81-72-684-6511 Tel: +81-72-684-7197

Short running title: Enhanced expression of autophagy and glycolysis markers in hypoxic keloid fibroblasts

Key words: Keywords: Autophagy, Fibroblasts, Glycolysis, Hypoxia, HIF, Keloid, Lactate, MCT4, Warburg effect

Abbreviations: HIF, hypoxia inducing factor; MCT, Monocarboxylate transporter; LDH, lactate dehydrogenase; LC3, Microtubule-associated protein-light chain 3

Summary

Keloid is a fibro-proliferative skin disorder with tumor-like behavior and dependence on anaerobic glycolysis (the Warburg effect), but its exact pathogenesis is unknown. Although autophagy is widely accepted as a lysosomal pathway for cell survival and cellular homeostasis (specifically upon exposure to stressors such as hypoxia), very few studies have investigated the involvement of autophagy and related glycolytic effectors in keloidogenesis. Here the authors examined the expression and cellular localization of autophagy proteins (LC3, pan-cathepsin), glycolytic markers (LDH, MCT1, MCT4) and the transcription factor HIF isoforms in human keloid samples using immunohistochemical analysis and double-labeling immunofluorescence methods. Based on H&E staining and expression of CD31, keloids were compartmentalized into hypoxic central and normoxic marginal zones. Vimentin-expressing fibroblasts in the central zone exhibited greater autophagy than their marginal-zone counterparts, as evidenced by increased LC3 puncta formation and co-localization with lysosomal pan-cathepsin. LDH (a lactate stimulator), MCT4 (a lactate exporter) and HIF-1 α expression levels were also higher in central-zone fibroblasts. Conversely, HIF-2 α expression was upregulated in fibroblasts and endothelial cells of the peripheral zone, while MCT1 was expressed in both zones. Taken together, these observations suggest that upregulation of autophagy and glycolysis markers in keloid hypoxic-zone fibroblasts may indicate a prosurvival mechanism allowing the extrusion of lactate to marginal-zone fibroblasts via metabolic coupling. The authors believe this is the first report on differential expression of autophagic and glycolytic markers in

keloid-zone fibroblasts. The study results indicate that autophagy inhibitors and MCT4 blockers may have therapeutic implications in keloid treatment.

Introduction

Autophagy is a prosurvival lysosomal pathway for degradation and recycling of damaged cellular components under normal conditions. However, it can become upregulated upon exposure to various stressors such as hypoxia, oxidative stress, mitochondrial dysfunction and inflammatory cytokines. Such an enhanced autophagic response can be antiapoptotic with clearance of damaged mitochondria and proteins, which are recycled for quality control and ATP synthesis (Kroemer et al., 2010; Galluzi et al., 2014; Narabayashi et al., 2015; Eid et al., 2016; Betsuyaku et al., 2017; Horibe et al., 2017). Morphologically, autophagy is characterized by the formation of LC3-mediated autophagosomes engulfing damaged material, which then fuse with lysosomes forming autolysosomes for cargo clearance and recycling. After synthesis, LC3 is cleaved to form cytoplasmic LC3-I, and upon induction of autophagy, LC3-I is lipidated to create LC3-II - the isoform responsible for autophagosome formation. LC3-II-mediated autophagosomes have been observed as puncta using immunohistochemical and immunofluorescence methods as recently reported by the authors (Narabayashi et al., 2015; Eid et al., 2016; Betsuyaku et al., 2017; Horibe et al., 2017) and others (Thomes et al., 2013).

In mouse models for breast cancer (Whitaker-Menezes et al., 2011; Chiavarina et al., 2012; Salem et al .2012) and human ovarian cancer (Thuwajit et al., 2017), oxidative stress and hypoxia (via HIF-1 α) were found to upregulate the expression of autophagy proteins (such as LC3-II) and glycolysis markers (such as LDH) in stromal fibroblasts, resulting in lactate overproduction and export by MCT4-overexpressing fibroblasts to adjacent MCT1-expressing cancer cells. Consequently, lactate production by autophagic hyperglycolytic fibroblasts stimulated the proliferation of cancer cells by what is called the reverse Warburg effect (via mitochondrial oxidative phosphorylation (OXPHOS) and lactate shuttling), distinguishing it from the original Warburg theory in cancer cells (Warburg, 1956; Martinez-Outschoorn et al., 2017). Knockdown of autophagy proteins (Atg5 or Beclin1) in cultured ovarian cancer-associated fibroblasts was seen to reduce LDH and MCT4 expression (Wang et al., 2016). This metabolic symbiosis or coupling involving lactate exporters and importers was also observed in the central hypoxic zone (glycolytic and MCT4-overexpressing) and the peripheral normoxic zone (highly proliferative and MCT1-expressing) of an in vivo colon cancer model (Adijanto and Philp 2012; Martinez-Outschoorn et al., 2017). Another example of metabolic symbiosis in normal tissue is the supply of anti-apoptotic lactate by adult Sertoli cells to proliferating germ cells via a Warburg-related glycolytic mechanism (Rato et al., 2016). Inhibition of autophagy in stressed cultured Sertoli cells using 3-methyladenine (3-MA) or lysosomal inhibitors decreased their viability and suppressed glycolysis, LDH formation and lactate

production, confirming the mutual relationship between autophagy and glycolysis and their survival roles (Bao et al., 2017; Horibe et al., 2017).

Keloids are locally aggressive, recurrent cutaneous fibro-proliferative masses characterized by excessive scarring and collagen formation. Their growth may be related to hypoxia, overexpression of cytokines and other factors (Jumper et al., 2015; Mari et al., 2015). The authors previously reported that keloid tissue exhibited high ATP levels even after around 10 years, perhaps due to anaerobic glycolysis (the Warburg effect) caused by hypoxia-related blood vessel flattening and crushing specifically in the central zone (Ueda et al., 1999, Kurokawa et al., 2010). However, the exact molecular mechanism of this vascular malformation is not clearly understood. Another study by the authors' research group showed that keloid nodules have distinct central hypoxic and marginal normoxic zones based on expression of CD31 (a marker of vascular endothelial cells) (Touchi et al., 2016). This CD31-based zonal division of keloid nodules is supported by a recent study (Chong et al.2015). keloid fibroblasts have bioenergetic characteristics similar to those of cancer cells, with generation of ATP mainly via glycolysis and possibly via induction of HIF-1 α and increased lactate production in hypoxic environments (Ueda et al., 1999, 2004; Vincent et al., 2008). Fibroblast heterogeneity is also a specific characteristic of keloids that governs their pathogenesis. Keloid fibroblasts (specifically those in the central zone) were found to be resistant to Fas-mediated apoptosis and quiescent, while those in the marginal zone of keloid scars exhibited higher production of collagen I and III as well as hyper-proliferation (Sayah et al., 1999; Lu et al., 2007 a, b; Syed et al., 2011; Li et al., 2013; Mari et al., 2015).

However, the exact molecular mechanisms of resistance to apoptosis in central-zone fibroblasts and production of excessive collagen with hyperproliferation in peripheral fibroblasts are not clearly understood.

As reported above, although autophagy has various prosurvival functions either alone or in conjunction with glycolysis (specifically under stress), there are very few studies that investigated autophagy in keloid pathogenesis. In addition, expression and localization of the lactate shuttle effectors MCT4 and MCT1 in addition to HIF-2 α (an essential protein for endothelial vessel integrity) (Skuli et al., 2009, 2012) in keloid nodules have not been reported on. Accordingly, the authors investigated the expression and specific cellular localization of autophagy proteins, glycolytic effectors and related transcription factor HIF isoforms (HIF-1 α and HIF-2 α) in keloid tissues using immunohistochemical and double-labeling immunofluorescence techniques.

Materials and Methods

Patients and samples

A total of 10 specimens resected at Osaka Medical College Hospital from January 2007 to December 2014 were selected for analysis. All the specimens were derived from patients diagnosed with keloids. The keloid nodules were resected from abdominal, thoracic, shoulder and neck regions. Clinical diagnosis here was based on the extension of scarring beyond the borders of the initial injury and variable pruritus, and was pathologically confirmed via microscopic identification of whorls consisting of haphazard hyalinized collagen bundles and a thick, flat epidermis.

None of the patients had undergone radiotherapy for keloids. The study was approved by the ethics committee of Osaka Medical College (no. 1892).

Histopathology

The specimens were fixed in 10% formalin, embedded in paraffin and cut into 5-μm sections for immunohistochemical analysis. Histological assessment was based on hematoxylin and eosin (H&E) staining by an independent pathologist.

Identification of keloid zones

Clinically, the central zone of each specimen was defined as the pale center of the keloid nodule, and the marginal zone was defined as area in which invasion of healthy tissue and erythema was evident on visual examination (Touchi et al 2016). Based on H&E staining, the central (hypoxic) zone of the nodules was defined as the part with few blood vessels, and the surrounding marginal (normoxic) zone was defined as a circular layer of collagen bundles rich in blood vessels. This zonal division was confirmed via CD31 immunohistochemical staining as outlined below.

Immunohistochemical analysis

Immunohistochemical analysis of the keloid samples was performed using paraffin-embedded sections as described here. The sections were deparaffinized, rehydrated and washed in phosphate-buffered saline (PBS). Antigen material was retrieved via treatment in 10 mM sodium citrate (pH 6.0) for 10 min. using a microwave oven. After a 10-min. period of incubation with 3% hydrogen peroxide, nonspecific antigens were blocked with 10% normal goat serum (Dako, CA, USA) for 20 min.

The sections were then incubated with primary antibodies (anti-LC3, rabbit polyclonal antibody (dilution: 1:1,000; MBL, Nagoya, Japan), anti-CD31, rabbit polyclonal antibody (1:25; Thermo Scientific, Waltham, MA), anti-LDH, rabbit polyclonal antibody (H-70) (1:100; Santa Cruz Biotechnology, Santa Cruz, CA), anti-MCT1, rabbit polyclonal antibody (H-160) (1:50; Santa Cruz), anti-MCT4, rabbit polyclonal antibody (H-90) (1:50; Santa Cruz), anti-HIF-1 α, mouse monoclonal (1:300; Novus Biologicals, Littleton, CO), anti-HIF-2 α, rabbit polyclonal antibody (1:50; Novus Bio.)) for an hour at 37℃. The sections were washed and incubated with a reagent containing goat anti-mouse and anti-rabbit immunoglobulins conjugated to peroxidase-labelled polymer (EnVision + System HRP kit, Dako, Tokyo, Japan) at room temperature for 30 min. The sections were examined after incubation using ImmPACT DAB Peroxidase (HRP) Substrate (Vector, Burlingame, CA). Counter staining was performed with hematoxylin (Wako, Osaka, Japan). Negative control on each slide was performed by replacing the primary antibody with either PBS or normal serum, corresponding to primary antibodies being used. For positive control, slides of normal rat testes and/or human ovarian cancer were stained, consistent with recent publications (Salem et al .2012; Rato et al., 2016; Horibe et al.2017; Martinez-Outschoorn et al., 2017; Thuwajit et al., 2017).

Single- and double-labeling immunofluorescence

The sections were deparaffinized, rehydrated and washed in PBS. Antigen material was retrieved via treatment in 10 mM sodium citrate (pH 6.0) for 10 min. using a microwave oven. After a 20-min. period of blocking with 3% bovine serum

albumin, the sections were incubated with primary antibodies (anti-LC3, mouse monoclonal antibody (dilution: 1:100; MBL), anti-LDH (1:100; Santa Cruz), anti-MCT1 (1:50; Santa Cruz), anti-MCT4 (1:50; Santa Cruz), anti-vimentin, goat polyclonal antibody (1:40; Sigma-Aldrich, St. Louis, MO, USA), anti-pan-cathepsin, goat polyclonal (1:50; Santa Cruz)) for an hour at room temperature. The sections were then washed in PBS and incubated with secondary antibodies (Alexa Fluor 594 chicken anti-rabbit or Alexa Fluor 488 donkey anti-goat (1:250; Life Technologies, Inc., Rockville, MO, USA) for 30 min. at room temperature. For double-labeling immunofluorescence, the sequential method previously reported by the authors (Narabayashi et al., 2015; Betsuyaku et al., 2017) was used. The samples were washed and mounted in Vectashield (Vector, Burlingame, CA) supplemented with 4',6-diamidino-2-phenylindole (DAPI) to enable visualization of nuclei. The labeled sections were observed with a confocal scanning laser microscope (TCS SP8, Leica, Germany).

Measurement procedure and selection of keloid nodules

A total of 35 collagen nodules was randomly chosen from 10 keloid samples with previously identified/evaluated central and marginal zones. Using Adobe Photoshop, images of either central or marginal zones of keloids were captured and saved for computer analysis. We used image J (National Institutes of Health, Bethesda, MA, USA) for quantitative immunohistochemical analysis of the two keloid zones by setting a "threshold", as previously reported by us and other researchers (Ito et al., 2006; Chong et al., 2015; Eid et al.;2016; Betsuyaku et al., 2017; Horibe etal.,2017). Under higher magnification, positive intensity was

detected, then at low power field, positive areas were captured and automatically calculated by the software (http://imagej.nih.gov/ij/).

Statistical analysis

Data analysis was performed using JMP 10.0 (SAS Institute, Cary, NC), with Student's t-test used to compare continuous variables between groups. P values of < 0.05 were considered statistically significant. Data here are expressed as means and standard deviations.

Results

Definition of central hypoxic and marginal normoxic zones in keloid nodules

Based on H&E keloid staining (Fig. 1 A), thin hyaline collagen fibers with deep eosinophilia were identified at the reticular layer of corium forming several spiral-shaped collagen nodules (marked by asterisks; Fig. 1 A a). As shown in Fig. 1 A b, these nodules were defined as central or hypoxic (less vascular; shown with a red line), and their peripheral parts were defined as marginal or normoxic (more vascular; area between red and blue lines) (Figs. 1 A b – e). Immunohistochemical analysis with anti-CD31 (an endothelial blood vessel marker) confirmed H&E staining and keloid zonation patterns. Enhanced expression of CD31 (Fig. 1 B) was observed in the marginal zone in contrast to very weak expression in central areas, and was statistically significant (Fig. 1 C).

Enhanced expression of autophagy and lysosomal proteins in central hypoxic keloid-zone fibroblasts

Immunohistochemical analysis (Figs. 2 A-a, b) and immunofluorescence (Fig. 2 B) labeling of LC3 (an essential autophagy marker) demonstrated enhanced expression with characteristic puncta or dot patterns (based on nuclear morphology) in central-zone fibroblasts in contrast to weaker expression in peripheral-zone fibroblasts, indicating enhanced autophagosome formation, and was statistically significant (Fig. 2 C) (Narabayashi et al., 2015; Eid et al., 2016; Betsuyaku et al., 2017; Horibe et al., 2017). Double-labeling immunofluorescence with vimentin (a fibroblast marker) and LC3 showed co-localization (Fig. 2D), indicating enhanced autophagy predominantly in fibroblasts. Importantly, double-labeling with pan-cathepsin (lysosomal marker) and LC3 showed enhanced expression and co-localization specifically in central-zone fibroblasts in contrast to weaker signals in marginal-zone fibroblasts (Fig. 2 E), indicating enhanced autolysosome formation and autophagic activity (Narabayashi et al., 2015; Eid et al., 2016 Betsuyaku et al., 2017; Horibe et al., 2017).

Upregulation of glycolysis and lactate export markers in keloid central-zone fibroblasts

To evaluate lactate production via glycolysis in keloids, immunohistochemical analysis using anti-LDH antibodies was performed (Figs. 3 A – C). The relative positive area of LDH was significantly higher in the central zone than in the marginal zone (Figs. 3 A, B). The double-labeling immunofluorescence of LDH

with vimentin showed co-localization, indicating that most LDH-expressing cells were specifically fibroblasts (Fig. 3 C). The expression of MCT4 (a lactate exporter) and MCT1 (a lactate importer) was also examined via immunohistochemical analysis (Fig. 4 A). Expression of MCT1 was observed in both keloid zones (Fig. 4 A a), while MCT4 was upregulated in the central zone (Fig. 4 A b). The relative positive areas of MCT4 were greater than MCT1-positive areas (Fig. 4 B). The histograms in Figs. 4 C and D clarify the immunohistochemical patterns of MCT1 and MCT4 shown in Figs. 4 A a and b. Comparison of differences between MCT1 and MCT4 positivity in individual collagen nodules indicates more MCT4-dominant nodules (62.9 vs. 37.1%; data not shown). As illustrated in Fig. 5, vimentin double-labeling immunofluorescence either with MCT1 (5 A) or MCT4 (5 B) showed enhanced co-localization, indicating that most MCT1- and MCT4-positive cells were fibroblasts.

Differential enhanced expression of HIF isoforms in keloid-zone fibroblasts

Immunohistochemical analysis with anti-HIF-1 α and anti-HIF-2 α antibodies in keloids was performed (Fig. 6). The nuclear expression of HIF-1 α was higher and more prevalent in central-zone fibroblasts (based on nuclear morphology) than in marginal-zone fibroblasts (Fig. 6 A), while nuclear HIF-2 α expression was higher in the marginal zone, specifically in fibroblasts and vascular endothelial cells (Fig. 6 B). This was confirmed via double-labeling immunofluorescence of HIF isoforms with vimentin (data not shown). However, the positive area for HIF-1 α was significantly larger than that for HIF-2 α (Fig. 6 C). Immunohistochemical statistical analysis of HIF-1 α and HIF-2 α is shown in the histograms of Figs. 6 D

and E, respectively. Positive cells for HIF-1 α were mostly located in the central zone (Fig. 6 D), while significantly more HIF-2 α-positive cells were found in the marginal zone (Fig. 6 E).

Discussion

The novel findings of the study were: 1) greater expression of autophagy proteins (LC3-II, pan-cathepsin), lactate exporter (MCT4) and HIF-1 α in central-zone fibroblasts than in marginal-zone fibroblasts; 2) greater expression of HIF-2 α in marginal-zone fibroblasts and endothelial cells than in the central zone; and 3) equal expression of MCT1 in both keloid zones. These findings are based on conventional H&E staining, statistical analysis, and immunohistochemical and double-labeling immunofluorescence techniques showing the expression and specific cellular localization of autophagy and glycolysis markers in keloid compartments.

In this study, observation under a light microscope indicated selectively enhanced autophagic response in central-zone fibroblasts as compared to the marginal zone based on a significant increase of LC3 puncta (evidence of autophagosome formation) and co-localization with overexpressed lysosomal pan-cathepsin, indicating the formation of autolysosomes and enhanced autophagic flux (Narabayashi et al., 2015; Eid et al., 2016; Betsuyaku et al., 2017; Horibe et al., 2017). The enhanced autophagy observed in central-zone fibroblasts could be an anti-apoptotic mechanism involving either the clearance of dysfunctional organelles such as mitochondria (Eid et al., 2016) or sequestration of caspase-8 in

autophagosomes, thus blocking the Fas-signaling pathway (Lu et al., 2007 a,b; Hou et al., 2010), and their recycling for lactate and other nutrients, resulting in ATP production (Kroemer et al., 2010; Galluzi et al., 2014; Martinez-Outschoorn et al., 2017). This may be supported by recent reporting indicating that autophagy activation is essential for fibroblast survival in long-lived mice (Wang and Miller, 2012), myofibroblast differentiation during the healing of human oral mucosa (Vescarelli et al., 2017) and promotion of fibrogenesis by hepatic stellate cells (Hernandez-Gea and Friedman, 2012). A recent study also showed that lactate may play a protective role for cultured skin fibroblasts against aging-related mitochondrial dysfunction via mitohormesis (Zelenka et al., 2015). The question of whether lactate may play a similar role for keloid fibroblasts requires further research. This enhanced autophagy in central-zone fibroblasts may also help to explain not only their resistance to apoptosis but also their specific features such as quiescence and longevity, reported in earlier studies (Sayah et al., 1999; Lu et al., 2007 a, b; Syed et al., 2011; Li et al., 2013; Tang and Rando, 2014). Importantly, the enhanced autophagy observed in hypoxic-zone fibroblasts in the current study may activate glycolysis and lactate production via enhanced expression of LDH and MCT4 as reported in relation to breast cancer-associated fibroblasts (Salem et al., 2012; Wang et al., 2016; Martinez-Outschoorn et al., 2017; Thuwajit et al., 2017). Collectively, the effects of autophagy may underpin the main survival mechanism orchestrating the regulation of stress responses, metabolic demand and cell proliferation in keloid fibroblasts.

The study also showed enhanced glycolytic activity in central-zone fibroblasts as demonstrated by enhanced expression of HIF-1 α, LDH and MCT4, in contrast to lower levels in the marginal zone. The enhanced autophagy and glycolysis observed in central-zone fibroblasts in the current study may be a mechanism by which lactate is provided to MCT1-expressing fibroblasts in the peripheral zone via metabolic coupling or lactate shuttling, allowing their proliferation and resulting in excessive collagen production and fibrogenic activity (Syed et al., 2011). The prosurvival metabolic coupling in keloid zones observed in the present study may be supported by recent studies indicating activity in solid tumors (between fibroblasts and cancer cells, or between hypoxic and normoxic cancer cells) (Whitaker-Menezes et al., 2011; Chiavarina et al., 2012; Adijanto and Philp 2012; Salem et al., 2012; Martinez-Outschoorn et al., 2017; Thuwajit et al., 2017) (as detailed in the Introduction section).

The upregulation of autophagy proteins and glycolysis markers observed in central-zone fibroblasts in the current study may be induced by hypoxia, as evidenced by enhanced expression of the transcriptional factor HIF-1 α (Ullah et al.2006; Martinez-Outschoorn et al., 2017; Chiavarina et al., 2012). However, hypoxia may activate autophagy via AMPK activity and LC3 -II induction independently of HIF-1 α and its target genes, BNIP3, and BNIP3L (Papandreou et al., 2008). Meanwhile, the authors' research group reported that expression of HIF-2 α (an essential factor for the survival, integrity and morphology of vascular endothelial cells and hyperproliferation via oxidative phosphorylation) (Hara et al.1999; Takahashi et al., 2004; Chiavarina et al., 2012; Skuli et al., 2009, 2012)

was lower in central-zone endothelial cells and fibroblasts than in the peripheral zone, consistent with CD31 expression. Recent studies have also shown that deletion of endothelial HIF-2 α in tumors resulted in tumor vessel collapse, abnormal morphology and fewer functional vessels (Skuli et al., 2009, 2012). It can therefore be inferred that the downregulation of HIF-2 α in the keloid central zone as observed in the current study may be linked to vascular flattening and crushing in this zone as previously reported by the authors (Ueda et al., 1999, 2004; Kurokawa et al.2010; Touchi et al.2016). Further research is needed to explore the mechanism of HIF-2 α downregulation in central keloid zone. Figure 7 summarizes the study's results and conclusions. The main limitation of this study was the relatively small sample size of surgically resected human keloids. Further experiments involving the use of cultured keloid fibroblasts and animal keloid models are needed to fully support the findings of the current work. These should include the use of electron microscopy, which is the most sensitive and revealing method for autophagy detection.

In conclusion, higher expression of autophagy proteins (LC3 and lysosomal pan-cathepsin) and glycolytic markers (HIF-1 α, LDH and MCT4) was observed in fibroblasts in the central hypoxic zone of collagen nodules than in normoxic peripheral-zone fibroblasts. This may allow autophagic fibroblasts in keloid hypoxic compartments to resist death signals and support the transfer of lactate to peripheral-zone fibroblasts, allowing them to proliferate with the subsequent persistence and longevity of keloids. An approach involving the targeting of fibroblasts in solid cancers using autophagy inhibitors (such as chloroquine) and/or

glycolysis inhibitors (such as AZ93) has been found to suppress the proliferation and metastasis of cancer epithelial cells (Martinez-Outschoorn et al.2017). As keloid fibroblasts behave like malignant cells in terms of proliferation, invasion and biological characteristics (Vincent et al., 2008; Mari et al., 2015), it can be inferred that autophagy inhibitors and MCT4 blockers may have therapeutic implications for keloid treatment.

References

Adijanto J. and Philp N.J. (2012). The SLC16A family of monocarboxylate transporters (MCTs)-physiology and function in cellular metabolism, pH homeostasis, and fluid transport. Curr. Top Membr. 70, 275-311.

Bao Z.Q., Liao T.T., Yang W.R., Wang Y., Luo H.Y. and Wang X.Z. (2017). Heat stress-induced autophagy promotes lactate secretion in cultured immature boar Sertoli cells by inhibiting apoptosis and driving SLC2A3, LDHA, and SLC16A1 expression. Theriogenology 87, 339-348.

Betsuyaku T., Eid N., Ito Y., Tanaka Y., Otsuki Y. and Kondo Y. (2017). Ethanol enhances thymocyte apoptosis and autophagy in macrophages of rat thymi. Histol. Histopathol. 32, 963-975.

Chiavarina B., Martinez-Outschoorn U.E., Whitaker-Menezes D., Howell A., Tanowitz H.B., Pestell R.G., Sotgia F. and Lisanti M.P. (2012). Metabolic reprogramming and two-compartment tumor metabolism; Opposing role(s) of

HIF1α and HIF2α in tumor-associated fibroblasts and human breast cancer cells. Cell Cycle 11, 3280-2389.

Chong Y, Park T.H, Seo S.W., and Chang C.H. (2015). Histomorphometric analysis of collagen architecture of auricular keloids in an Asian population. Dermatol. Surg. 41, 415-22.

Eid N., Ito Y., Horibe A. and Otsuki Y. (2016). Ethanol-induced mitophagy in liver is associated with activation of the PINK1-Parkin pathway triggered by oxidative DNA damage. Histol. Histopathol. 31, 1143-1159.

Galluzzi L., Pietrocola F., Levine B. and Kroemer G. (2014). Metabolic control of autophagy. Cell 159, 1263-1276.

Hara S., Kobayashi C. and Imura N. (1999). Nuclear Localization of Hypoxia-Inducible Factor-2α in Bovine Arterial Endotherial Cells. Mol. Cell Biol. Res. Commun. 2, 119-123.

Hernandez-Gea V. and Friedman S.L. (2012). Autophagy fuels tissue fibrogenesis. Autophagy 8, 849-850.

Horibe A., Eid N., Ito Y., Hamaoka H., Tanaka Y. and Kondo Y. (2017). Upregulated Autophagy in Sertoli Cells of Ethanol-Treated Rats Is Associated with Induction of Inducible Nitric Oxide Synthase (iNOS), Androgen Receptor Suppression and Germ Cell Apoptosis. Int. J. Mol. Sci. 18. pii: E1061. doi: 10.3390/ijms18051061.

Hou W., Han J., Lu C., Goldstein L.A. and Rabinowich H. (2010). Autophagic degradation of active caspase-8: a crosstalk mechanism between autophagy and apoptosis. Autophagy 6, 891-900.

Ito Y., Shibata M.A., Kusakabe K. and Otsuki Y. (2006). Method of specific detection of apoptosis using formamide-induced DNA denaturation assay. J. Histochem. Cytochem. 54, 683-692.

Jumper N., Paus R. and Bayat A. (2015). Functional histopathology of keloid disease. Histol. Histopathol. 30, 1033-1057.

Kurokawa N., Ueda K. and Tsuji M. (2010). Study of microvascular structure in keloid and hypertrophic scars: density of microvessels and the efficacy of three-dimensional vascular imaging. J. Plast. Surg. Hand Surg. 44, 272-277.

Kroemer G., Marino G. and Levine B. (2010). Autophagy and the integrated stress response. Mol. Cell 40, 280-293.

Li H., Nahas Z., Feng F, Elisseeff J.H. and Boahene K. (2013). Tissue engineering for in vitro analysis of matrix metalloproteinases in the pathogenesis of keloid lesions. JAMA Facial Plast. Surg. 15, 448-456.

Lu F., Gao J, Ogawa R, Hyakusoku H. and Ou C. (2007a). Fas-mediated apoptotic signal transduction in keloid and hypertrophic scar. Plast. Reconstr. Surg. 119, 1714-1721.

Lu F., Gao J., Ogawa R., Hyakusoku H. and Ou C. (2007b). Biological differences between fibroblasts derived from peripheral and central areas of keloid tissues. Plast. Reconstr Surg. 120, 625-630.

Mari W., Alsabri S.G., Tabal N., Younes S., Sherif A. and Simman R. (2015). Novel Insights on Understanding of Keloid Scar: Article Review. J. Am. Coll. Clin. 7, 1-7.

Martinez-Outschoorn U.E., Peiris-Pages M., Pestell R.G., Sotgia F. and Lisanti MP. (2017). Cancer metabolism: a therapeutic perspective. Nat. Rev. Clin. Oncol. 14, 11-31.

Narabayashi K., Ito Y., Eid N., Maemura K., Inoue T., Takeuchi T., Otsuki Y. and Higuchi K. (2015). Indomethacin suppresses LAMP-2 expression and induces lipophagy and lipoapoptosis in rat enterocytes via the ER stress pathway. J. Gastroenterol. 50, 541-554.

Papandreou I., Lim A.L, Laderoute K. and Denko NC. (2008). Hypoxia signals autophagy in tumor cells via AMPK activity, independent of HIF-1, BNIP3, and BNIP3L. Cell Death Differ. 15, 1572-1581.

Rato L., Meneses M.J., Silva B.M., Sousa M., Alves M.G. and Oliveira P.F. (2016). New insights on hormones and factors that modulate Sertoli cell metabolism. Histol. Histopathol. 31, 499-513.

Salem A.F., Whitaker-Menezes D., Lin Z., Martinez-Outschoorn U.E., Tanowitz H.B., Al-Zoubi M.S., Howell A., Pestell R.G., Sotgia F. and Lisanti M.P. (2012).

Two-compartment tumor metabolism: autophagy in the tumor microenvironment and oxidative mitochondrial metabolism (OXPHOS) in cancer cells. Cell Cycle 11, 2545-2556.

Sayah D.N., Soo C., Shaw W.W., Watson J, Messadi D, Longaker M.T., Zhang X. and Ting K. (1999). Downregulation of apoptosis-related genes in keloid tissues. J. Surg. Res. 87, 209-216.

Skuli N., Liu L., Runge A., Wang T., Yuan L., Patel S., Iruela-Arispe L., Simon M.C. and Keith B. (2009). Endothelial deletion of hypoxia-inducible factor-2alpha (HIF-2alpha) alters vascular function and tumor angiogenesis. Blood 114, 469-477.

Skuli N., Majmundar A.J., Krock B.L., Mesquita R.C, Mathew L.K., Quinn Z.L., Runge A, Liu L., Kim M.N., Liang J., Schenkel S, Yodh A.G., Keith B. and Simon M.C. (2012). Endothelial HIF-2α regulates murine pathological angiogenesis and revascularization processes. J. Clin. Invest. 122, 1427-1443.

Syed F., Ahmadi E., Iqbal S.A., Singh S., McGrouther D.A. and Bayat A. (2011). Br J Dermatol. 164, 83-96. Fibroblasts from the growing margin of keloid scars produce higher levels of collagen I and III compared with intralesional and extralesional sites: clinical implications for lesional site-directed therapy. Br. J. Dermatol. 164, 83-96.

Takahashi R., Kobayashi C., Kondo Y., Nakatani Y., Kudo I., Kunimoto M., Imura N. and Hara S. (2004). Subcellular localization and regulation of hypoxia-inducible factor-2α in vascular endothelial cells. Biochem. Biophys. Res. Commun. 317, 84-91.

Tang A.H. and Rando T.A. (2014). Induction of autophagy supports the bioenergetic demands of quiescent muscle stem cell activation. EMBO J. 33, 2782-2789.

Thomes P.G., Ehlers R.A., Trambly C.S., Clemens D.L., Fox H.S., Tuma D.J. and Donohue T.M. (2013). Multilevel regulation of autophagosome content by ethanol oxidation in HepG2 cells. Autophagy 9, 63-73

Thuwajit C., Ferraresi A., Titone R., Thuwajit P. and Isidoro C. (2017). The metabolic cross-talk between epithelial cancer cells and stromal fibroblasts in ovarian cancer progression: Autophagy plays a role. Med. Res. Rev. doi: 10.1002/med.21473. [Epub ahead of print].

Touchi R., Ueda K., Kurokawa N. and Tsuji M. (2016). Central regions of keloids are severely ischemic. J. Plast. Reconstr. Aesthet. Surg.69, 35-41.

Ueda K., Furuya E., Yasuda Y., Oba S., Tajima S. (1999). Keloids have continuous high metabolic activity. Plast. Reconstr. Surg. 104, 694-698.

Ueda K., Yasuda Y., Furuya E., Oba S. (2004) Inadequate blood supply persists in keloids. Scand. J. Plast. Reconstr. Surg. Hand Surg. 38, 267-271.

Ullah M.S., Davies A.J. and Halestrap A.P. (2006). The Plasma membrane lactate transporter MCT4, but not MCT1, is up-regulated by hypoxia through a HIF-1α-dependent mechanism. J. Biol. Chem. 281, 9030-0937.

Vescarelli E., Pilloni A., Dominici F., Pontecorvi P., Angeloni A., Polimeni A., Ceccarelli S. and Marchese C. (2017). Autophagy activation is required for

myofibroblast differentiation during healing of oral mucosa. J. Clin. Periodontol. 44, 1039-1050.

Vincent A.S., Phan T.T., Mukhopadhyay A., Lim H.Y., Halliwell B. and Wong K.P. (2008). Human skin keloid fibroblasts display bioenergetics of cancer Ccells. J. Invest. Dermatol. 128, 702-709.

Wang M. and Miller R.A. (2012). Fibroblasts from long-lived mutant mice exhibit increased autophagy and lower TOR activity after nutrient deprivation or oxidative stress. Aging Cell 2012 11, 668-674.

Wang Q., Xue L., Zhang X., Bu S., Zhu X. and Lai D. (2016). Autophagy protects ovarian cancer-associated fibroblasts against oxidative stress. Cell Cycle. 18, 1376-1385.

Warburg O. On the Origin of cancer cells. (1956). Science 123, 309-314.

Whitaker-Menezes D, Martinez-Outschoorn UE, Lin Z, Ertel A, Flomenberg N, Witkiewicz A.K., Birbe R.C., Howell A., Pavlides S., Gandara R., Pestell R.G., Sotgia F., Philp N.J. and Lisanti M.P. (2011). Evidence for a stromal-epithelial "lactate shuttle" in human tumors: MCT4 is a marker of oxidative stress in cancer-associated fibroblasts. Cell Cycle 10, 1772-1783.

Zelenka J., Dvořák A. and Alán L. (2015). L-Lactate Protects Skin Fibroblasts against Aging-Associated Mitochondrial Dysfunction via Mitohormesis. Oxid. Med. Cell Longev. 2015, 351698. doi: 10.1155/2015/351698.

Figure legend

Fig. 1. Central (hypoxic) and marginal (normoxic) keloid zones. A: H&E staining of keloid nodules at low magnification (asterisks) and magnified (b – e). E, epidermis. The keloid central zone (CZ) and marginal zone (MZ) (b) are identified by red and blue circular lines. A higher magnification of the keloid zones in c (framed areas) is shown in d and e. Arrows in e indicate blood vessels in the marginal zone. B: Immunohistochemical analysis of CD31 in keloid zones. CD31 expression in endothelial cells was more marked in the marginal zone (red arrow heads) than in the central zone with statistical significance C: *P < 0.0001. Black arrow heads indicate the outer limiting border of keloid nodule The inset in B is a magnification of the framed area.

Fig. 2. Enhanced expression of autophagy proteins in hypoxic-zone fibroblasts. A a, b: Immunohistochemical analysis of LC3 (an autophagosome marker) in keloid zones at low magnification and related expression in the central zone (a) (arrow heads). The higher magnification in b shows the dot-like pattern of LC3-II in cells with fibroblast-like morphology (based on nuclear shape) (black arrows) (magnified in inset). B: Immunofluorescence staining of LC3-II puncta (white arrows) and quantification in keloid zones. C: *P < 0.0005. D: Double-labeling immunofluorescence for LC3 (red) with vimentin (a fibroblast marker) (green). The framed areas are magnified on the right to show enhanced co-localization upon mergence (arrows) (yellow). E: Double-labeling immunofluorescence for LC3 (red) with pan-cathepsin (a lysosomal marker) (green). The framed area is magnified on the right to show enhanced co-localization upon mergence (arrows) (yellow).

Fig. **3**. LDH expression upregulated in central-zone fibroblasts. A: Immunohistochemical analysis of LDH and quantification. B: Statistically significant increase of LDH expression in the central zone (arrow heads show keloid nodule borders) (*P < 0.0001). C: Double-labeling immunofluorescence for LDH (red) with vimentin (green). The LDH-positive area is overlapped with vimentin signals and appears yellow upon mergence (arrows).

Fig. **4**. Immunohistochemical analysis for MCT1 and MCT4 in keloid zones demonstrating selective upregulation of MCT4 in the hypoxic zone. MCT1-positive areas (Fig. 4 A a) are expressed moderately in both nodule zones, while MCT4 (Fig. 4 b) is overexpressed specifically in the central zone. Arrow heads indicate the keloid nodule border. The histograms in B – D show immunohistochemical quantitative analysis.

Fig. **5**. MCT4 and MCT1 expression is predominantly seen in keloid-zone fibroblasts. Double-labeling immunofluorescence for vimentin (green) with either MCT1 (Fig. 5 A) or MCT4 (Fig. 5 B) (red) showed enhanced co-localization in fibroblasts (arrows, yellow).

Fig. 6. Immunohistochemical analysis for HIF-1 α and HIF-2 α showed differential expression in keloid zones (large arrow heads indicate the keloid nodule border). HIF-1 α expression was mostly detected in the central zone of collagen nodules. A: In fibroblasts (based on nuclear morphology; long arrows in the magnified figure on the right). The divided arrows indicate nuclear expression. (B) HIF-2 α expression is mostly observed in the marginal zone. The magnified figure on the

right shows expression in fibroblasts (small arrow heads) and endothelial cells (arrows) of blood vessels (asterisks mark the lumen of blood vessels). The histograms in C – E show immunohistochemical statistical analysis. *P < 0.0001 in C and 0.37 in E.

Fig. 7. Main achievements/findings of the current study and implications for keloidogenesis. A: Categorization of keloid central (hypoxic) and marginal (normoxic) zones based on expression of CD31, HIF-1 α and HIF-2 α (hypoxic- and marginal-zone fibroblasts express HIF-1 α and HIF-2 α, respectively, while vascular endothelial cells in the peripheral zone express both CD31 and HIF-2 α, as shown and detailed in B). B: Enhanced expression of autophagy markers (LC3-II and lysosomal pan-cathepsin) and glycolytic markers (LDH and MCT4) in hypoxic central-zone fibroblasts may be mediated by HIF-1 α, and may be a prosurvival mechanism. It may also stimulate lactate exportation to MCT1-expressing fibroblasts in the marginal zone for proliferation via lactate shuttling (metabolic symbiosis, or the reverse Warburg effect), thus supporting the tumor-like behavior, invasion and persistence of keloids.

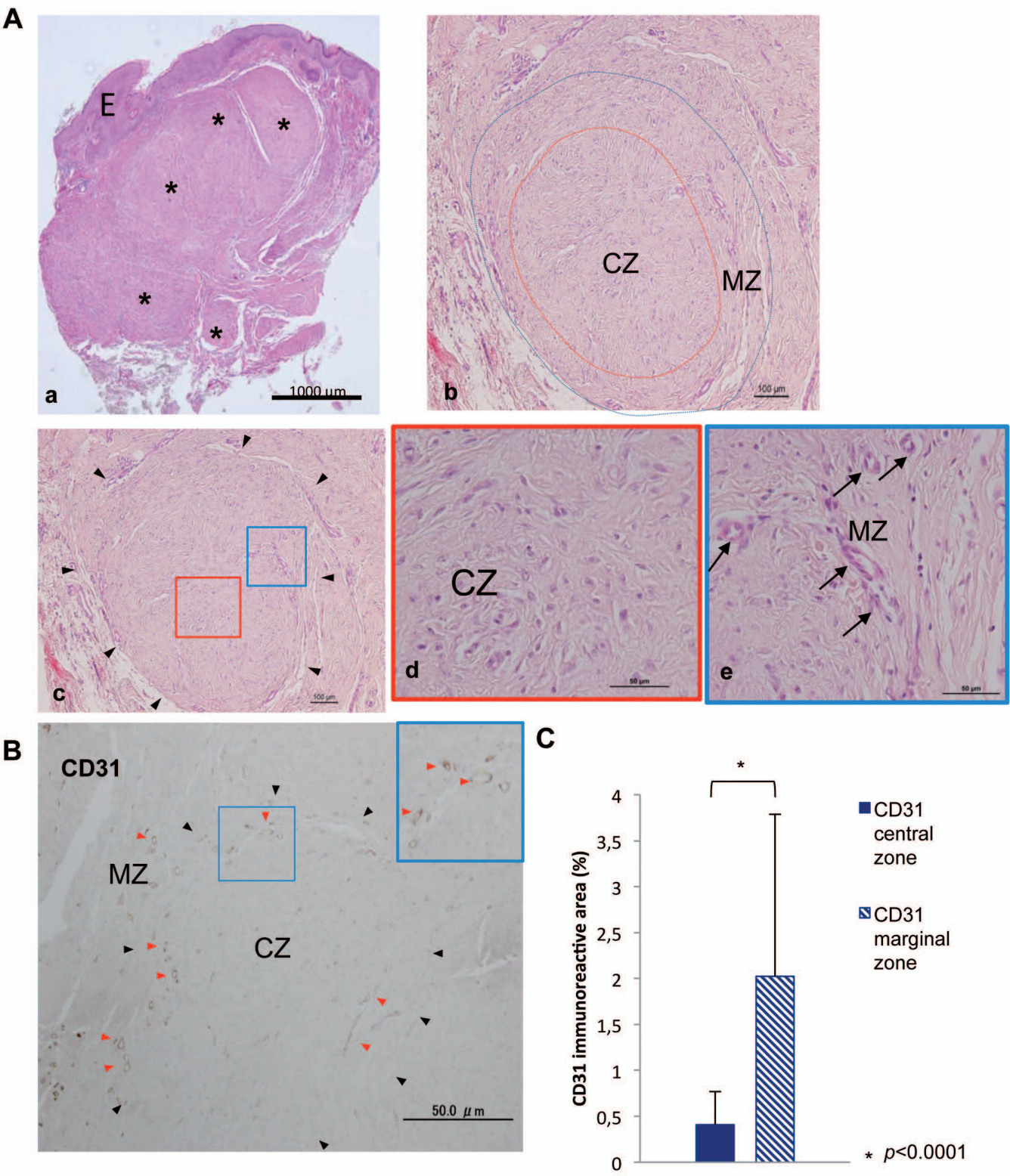
A
E
a
1000 µm
b
CZ
MZ
100 µm
c
100 µm
d
CZ
50 µm
e
MZ
50 µm
B
CD31
MZ
CZ
50.0 µm
C
CD31 immunoreactive area (%)
4
3,5
3
2,5
2
1,5
1
0,5
0
*
CD31 central zone
CD31 marginal zone
* p<0.0001

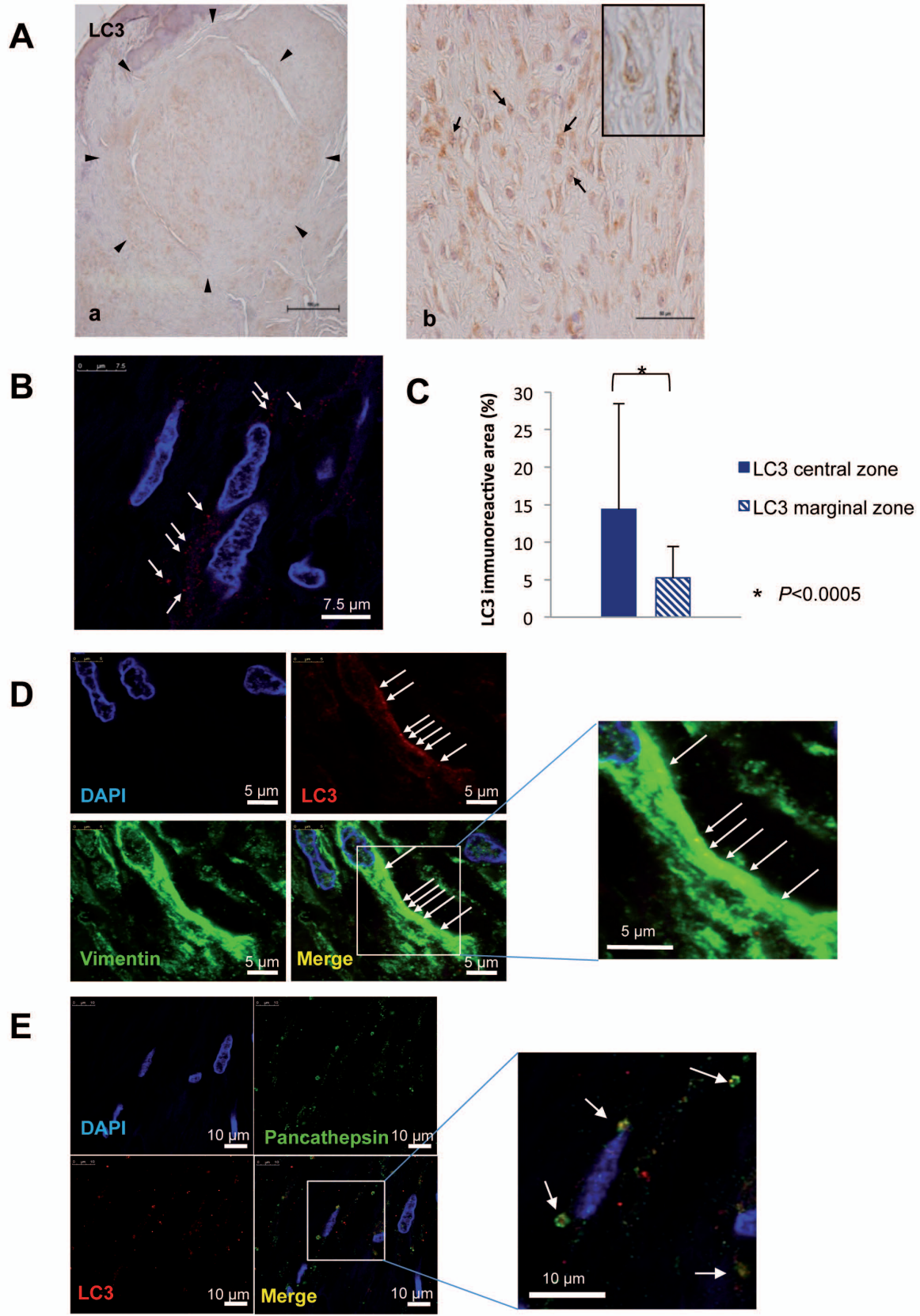
A
LC3
a
b
B
7.5 µm
C
LC3 immunoreactive area (%)
30
25
20
15
10
5
0
*
LC3 central zone
LC3 marginal zone
* P<0.0005
D
DAPI
5 µm
LC3
5 µm
Vimentin
5 µm
Merge
5 µm
5 µm
E
DAPI
10 µm
Pancathepsin
10 µm
LC3
10 µm
Merge
10 µm
10 µm

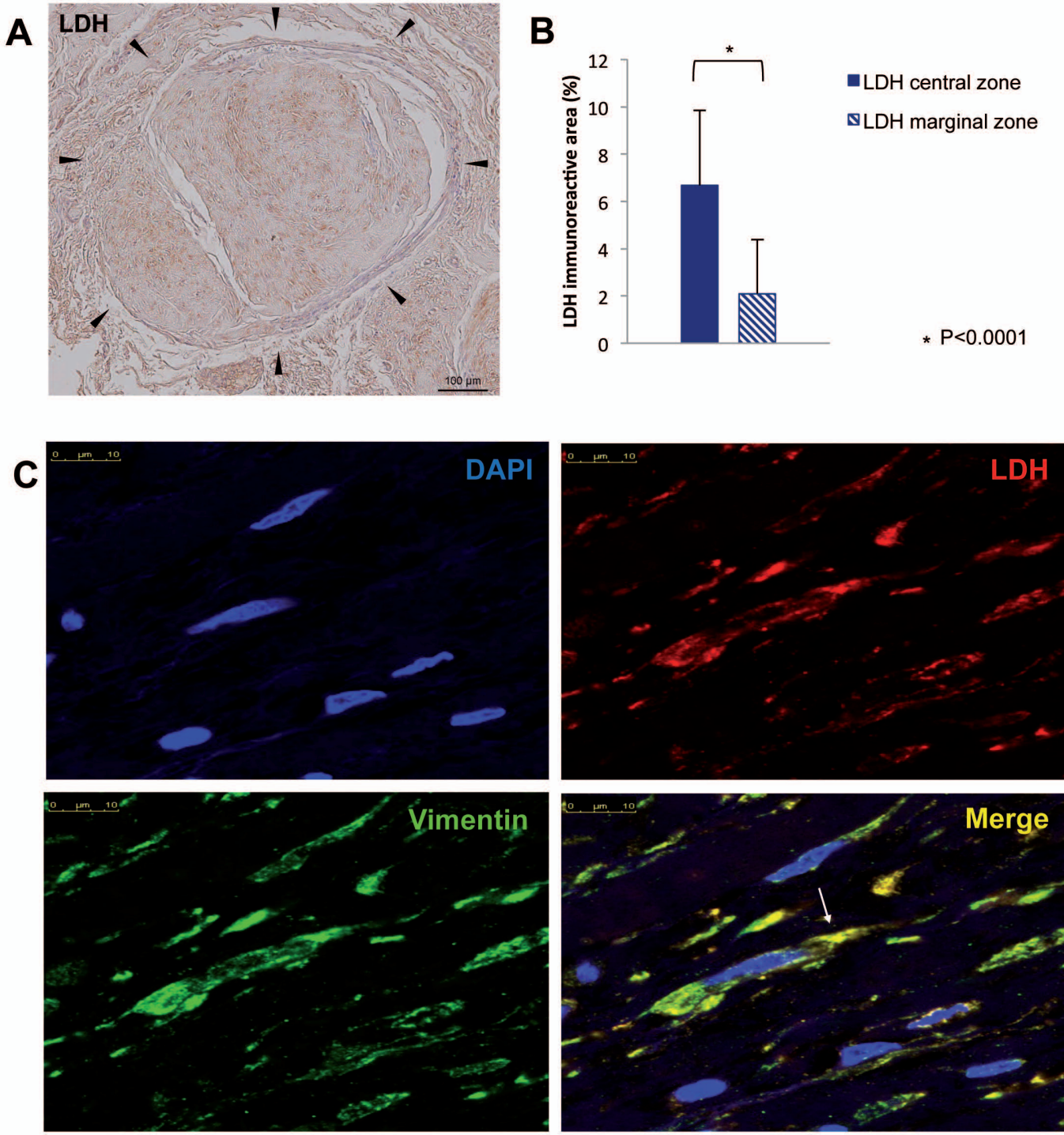
A
LDH
100 µm
B
LDH immunoreactive area (%)
12
10
8
6
4
2
0
*
LDH central zone
LDH marginal zone
* P<0.0001
C
DAPI
LDH
Vimentin
Merge

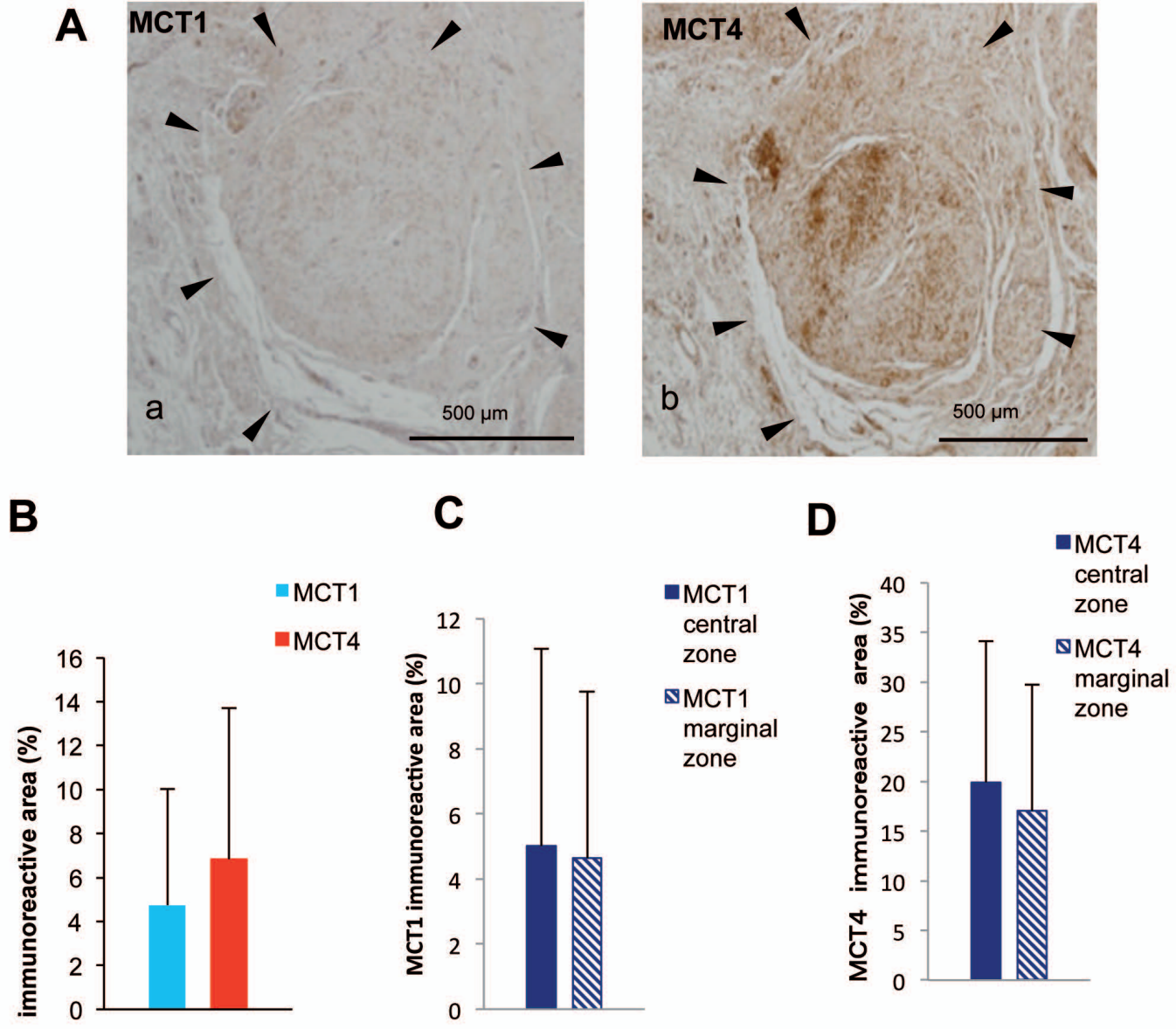
A
MCT1
a
500 µm
MCT4
b
500 µm
B
MCT1
MCT4
immunoreactive area (%)
0
2
4
6
8
10
12
14
16
C
MCT1 central zone
MCT1 marginal zone
MCT1 immunoreactive area (%)
0
2
4
6
8
10
12
D
MCT4 central zone
MCT4 marginal zone
MCT4 immunoreactive area (%)
0
5
10
15
20
25
30
35
40

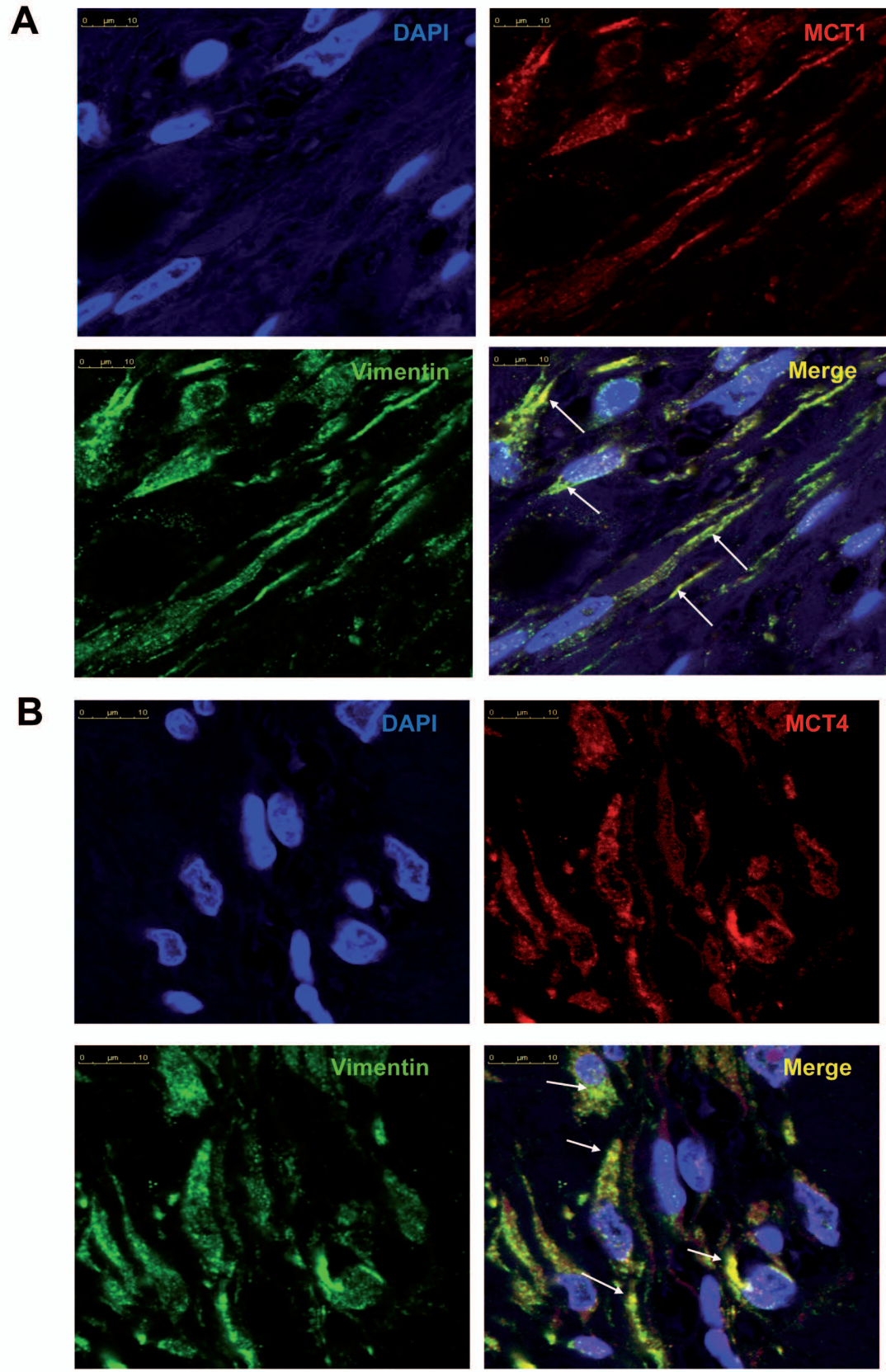
A
DAPI
MCT1
Vimentin
Merge
B
DAPI
MCT4
Vimentin
Merge

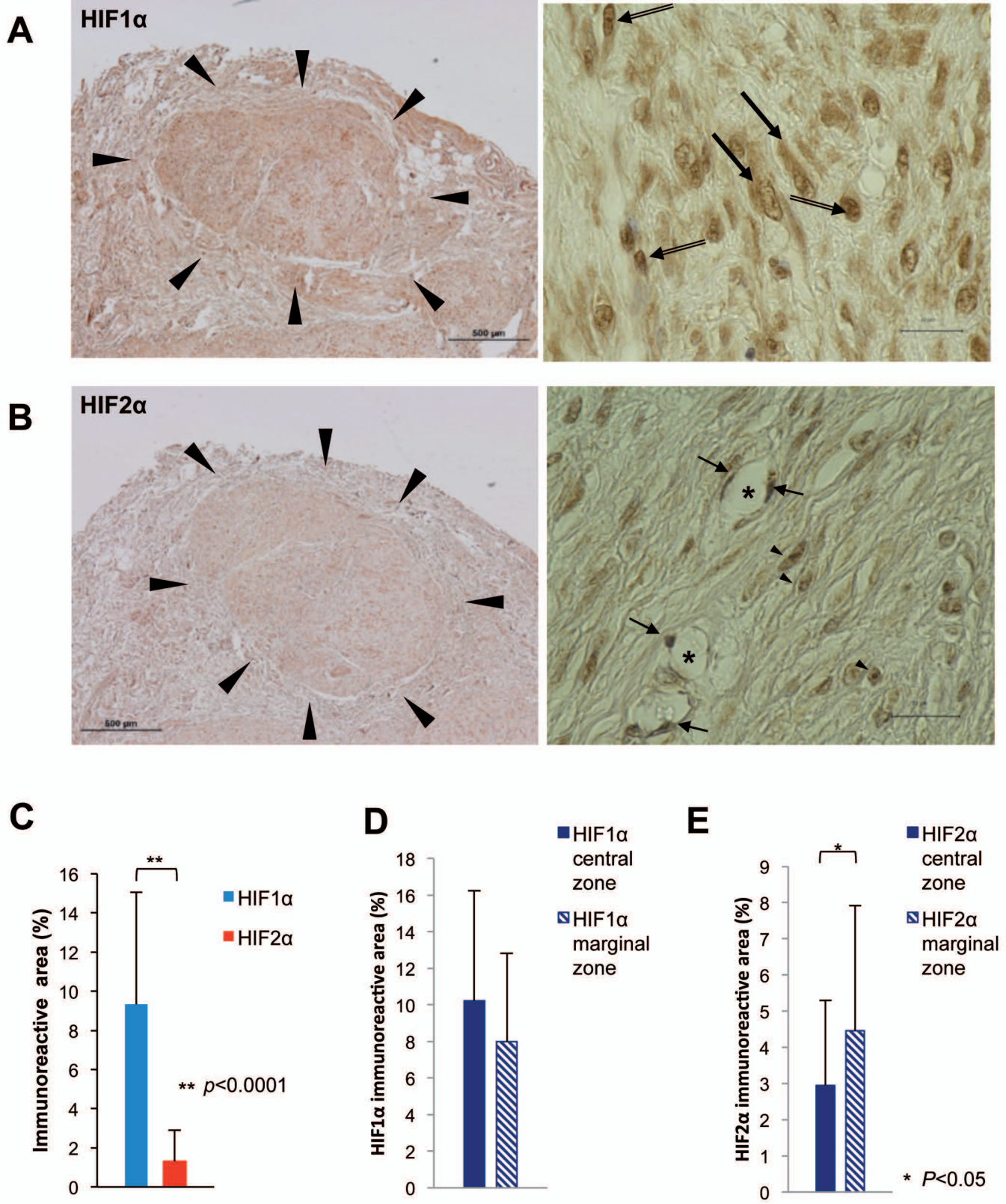
A
HIF1α
500 μm
B
HIF2α
500 μm
C
Immunoreactive area (%)
16
14
12
10
8
6
4
2
0
**
HIF1α
HIF2α
** p<0.0001
D
HIF1α immunoreactive area (%)
18
16
14
12
10
8
6
4
2
0
HIF1α central zone
HIF1α marginal zone
E
HIF2α immunoreactive area (%)
9
8
7
6
5
4
3
2
1
0
*
HIF2α central zone
HIF2α marginal zone
* P<0.05

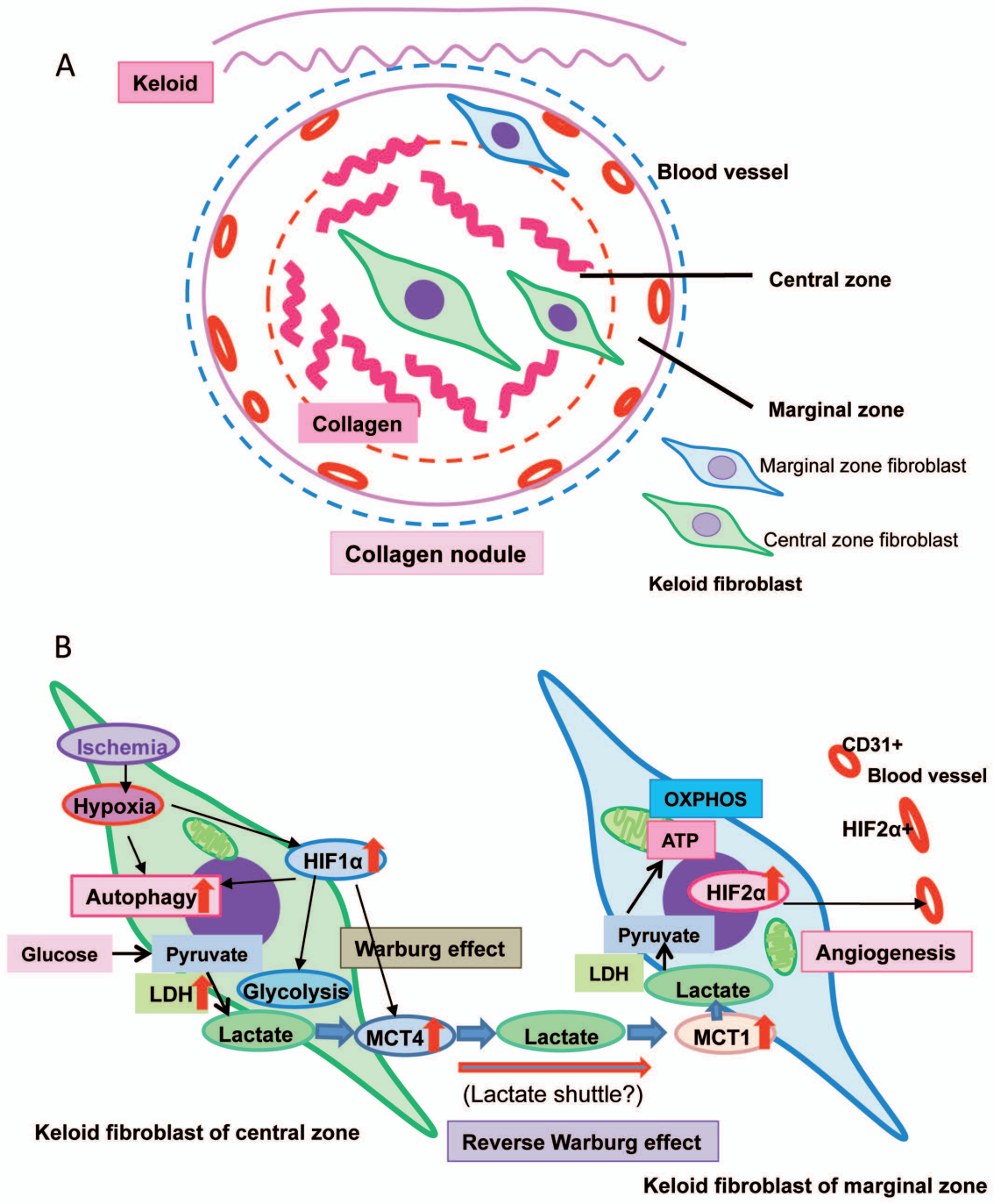
A
Keloid
Blood vessel
Central zone
Marginal zone
Collagen
Marginal zone fibroblast
Central zone fibroblast
Collagen nodule
Keloid fibroblast
B
Ischemia
Hypoxia
HIF1α
Autophagy
Glucose
Pyruvate
Warburg effect
LDH
Glycolysis
Lactate
MCT4
Lactate
(Lactate shuttle?)
Keloid fibroblast of central zone
Reverse Warburg effect
CD31+
Blood vessel
OXPHOS
ATP
HIF2α+
HIF2α
Pyruvate
Angiogenesis
LDH
Lactate
MCT1
Keloid fibroblast of marginal zone